Available online at www.sciencedirect.com
SCIENCE DIRECT®
Experimental Eye Research 77 (2003) 515–524
EXPERIMENTAL EYE RESEARCH
www.elsevier.com/locate/yexer

Involvement of corneal nerves in the progression of keratoconus

N.H. Brookes[a], I.-P. Loh[a], G.M. Clover[a], C.A. Poole[b], T. Sherwin[a,*]

[a]*Department of Ophthalmology, Faculty of Medicine and Health Sciences, University of Auckland, Private Bag 92019, Auckland, New Zealand*
[b]*Department of Anatomy and Radiology, University of Auckland, Auckland, New Zealand*

Received 18 November 2002; accepted in revised form 22 May 2003

Abstract

Keratoconus is a debilitating corneal thinning disease that principally develops in the second and third decades of life. Our group previously developed a novel approach to studying keratoconus, based on the observation that there is a gradient of damage across the keratoconic cone.

We identified a number of cellular characteristics of keratoconus such as discrete incursions of fine cellular processes from the anterior keratocytes in association with localised indentation of the basal epithelium, and increased levels of the lysosomal enzymes Cathepsin B and G in aberrant keratocytes, located beneath compromised regions of Bowman's layer, but also deeper in the stroma. Enzyme activity by these cells seemed to be causing localised structural degradation of the anterior stroma, leading to near-complete destruction of both Bowman's layer and the stroma, often necessitating a full-thickness corneal graft for sight restoration.

This current study extends our initial findings by investigating the role of corneal nerves passing between the stroma and epithelium at the sites of early degradative change observed previously, and may be facilitating the keratocyte–epithelial interactions in this disease.

Cells in sections of normal and keratoconic human corneas were labelled with the fixable fluorescent viability dye 5-chloromethylfluorescein diacetate, antibodies to α-tubulin (nerves), α3β1 integrin, Cathepsin B and G, and the nuclear dye DAPI, and then examined with a confocal microscope. Anterior keratocyte nuclei were seen wrapping around the nerves as they passed through the otherwise acellular Bowman's layer, and as the disease progressed and Bowman's layer degraded, these keratocytes were seen to express higher levels of Cathepsin B and G, and become displaced anteriorly into to the epithelium. Localised nerve thickenings also developed within the epithelium in association with Cathepsin B and G expression, and appeared to be very destructive to the cornea.

Insight into the molecular mechanisms of keratoconic disease pathogenesis and progression can be gained from the process of extracellular matrix remodelling known from studies of connective tissues other than the cornea, and wound healing studies in the cornea. Further studies are required to determine how well this model fits the actual molecular basis of the pathogenesis of keratoconus.

Keywords: cornea; keratoconus; nerve; pathogenesis; confocal microscopy; immunohistochemistry

1. Introduction

Keratoconus is a debilitating corneal ectasia that principally affects young people in the second or third decade of their lives.

In recent years, there has been a large amount of literature published on keratoconus. However, most of this concerns the surgical management of patients with the disease, rather than exploring the mechanism of the disease process itself (for a review see Rabinowitz, 1998).

In a previous study (Sherwin et al., 2002), our group developed a novel approach to studying keratoconus, based on our observation that there is a gradient of damage between the central (most damage/least normal) and peripheral (least damaged/most normal) parts of the keratoconic cone. We hypothesised that the peripheral parts of the cone exhibited the earliest morphological and biochemical signs of keratoconic pathogenesis.

In this earlier study we identified a number of cellular characteristics of keratoconus. Firstly, we observed discrete incursions of fine cellular processes from the anterior keratocytes, often in association with a localised indentation of the basal epithelium. Secondly, we measured increased levels of the lysosomal enzymes Cathepsin B and G in

* Corresponding author. T. Sherwin. Department of Ophthalmology, Faculty of Medicine and Health Sciences, University of Auckland, Private Bag 92019, Auckland, New Zealand.
E-mail address: t.sherwin@auckland.ac.nz (T. Sherwin).

0014-4835/03/$ - see front matter © 2003 Elsevier Ltd. All rights reserved.
DOI:10.1016/S0014-4835(03)00148-9

aberrant keratocytes, mostly located posteriorly to compromised regions of Bowman's layer, but also deeper in the stroma. These findings are in stark contrast to our understanding of keratocyte connectivity in the normal cornea, where the cells act as a highly coupled network, rather than as isolated cells or cell clusters (Nishida et al., 1988; Poole et al., 1993; Jester et al., 1994; Watsky, 1995; Poole et al., 1996; Clover et al., 1996a,b; Petridou and Masur, 1996; Müller et al., 1996; Clover et al., 1998; Snyder, 1998; Spanakis et al., 1998; Hahnel et al., 2000; Ojeda et al., 2001).

We hypothesised that it was degradative enzyme activity from these abnormal cells that was causing localised structural degradation of both Bowman's layer and the stroma, which may be further exacerbated by physical stresses such as intraocular pressure and eye rubbing. These changes ultimately lead to near-complete destruction of both Bowman's layer and the stroma, often necessitating a full-thickness corneal graft (penetrating keratoplasty) for sight restoration.

This current study explores a further feature of the progression of keratoconus, extending our initial findings by investigating the role of corneal nerves passing between the stroma and epithelium at the sites of early degradative change observed previously.

The cornea is densely innervated by sensory fibres from the ophthalmic branch of the trigeminal nerve, which respond to mechanical, thermal and chemical stimulation of the cornea. Individual nerve cells communicate via a range of both classical and peptidergic neurotransmitters. In the human cornea, many radially oriented nerve bundles enter the cornea via the sclera in the 9–3 hr direction, bend 90° and pass through Bowman's layer, then bend 90° again, before ramifying and ending within the epithelium as free nerve endings (mostly C-fibres) (Scharenberg, 1955; Tervo, 1977; Marfurt and Ellis, 1993; Müller et al., 1995, 1996, 1997).

In the human cornea, nerve fibres are the only cellular entities crossing the otherwise acellular Bowman's layer. This current study aims to explore the relationship between these nerves and the features of keratoconus identified in our earlier study (Sherwin et al., 2002).

2. Materials and methods

2.1. Tissue source and dissection

This study used human corneal tissue from two distinct sources, both with ethical consent formally approved by the Auckland Human Subjects Ethics Committee.

Normal post-mortem tissue was obtained from The New Zealand National Eye Bank, when it was not transplantable because the donor age or post-mortem interval fell outside the acceptance criteria.

Diseased keratoconic buttons were obtained at the time of restorative corneal grafting.

An 8 mm trephine was used to remove a central corneal button from the normal corneas. These normal buttons, along with the keratoconic buttons obtained at surgery were cut into three equal parts with a razor blade.

2.2. Keratocyte labelling and sectioning

The tissue pieces were left to label the keratocytes overnight at room temperature in the fluorescent viability probe CellTracker-Green (5-chloromethylfluorescein diacetate (CMFDA); Molecular Probes, Inc., USA) and Corneal Transport Medium (CTM; high-osmolar Minimum Essential Medium: Armitage and Moss, 1990). The next day, the tissue was washed in CTM, fixed for 15 min in 2·5% Paraformaldehyde in Phosphate Buffered Saline (pH 7·4), then washed again, before storing in CTM with 20% Dimethyl Sulphoxide at −80°C (Poole et al., 1995).

When needed, the tissue pieces were thawed to room temperature, then washed several times in CTM, before being mounted and frozen in OCT (TissueTek, USA). Multiple 30 μm sections were then cut from each block in an antero-posterior orientation, and dried overnight, at room temperature in the dark, onto pre-prepared glass slides coated with poly-L-lysine (Sigma, USA).

2.3. Immunohistochemistry

Combinations of the same panel of antibodies used in our previous study (Sherwin et al., 2002) were applied to the tissue sections, as detailed in Table 1.

Each section was labelled first with the acetylated α-tubulin antibody (C3B9) detected with an Alexa-546 probe, and then labelled with antibodies to either Cathepsin B, Cathepsin G, or α3β1 integrin, detected with a Cy5 probe. Most slides were finally labelled with the intercalating DNA

Table 1
List of antibodies

Antibody	Description	Source
Acetylated α-tubulin (C3B9)	Mouse monoclonal	Woods et al. (1989)
Cathepsin B	Sheep anti-human	Serotec #AHP18H
Cathepsin G	Mouse monoclonal	ICN Biomedicals #64-732
α3β1 Integrin	Mouse monoclonal anti-human	DAKO #M608
Goat anti-mouse IgG Alexa-546	Fluorescent secondary antibody	Molecular probes #A11003
Biotinylated donkey anti-sheep IgG	Biotinylated secondary antibody	Sigma #7390
Biotinylated goat anti-mouse IgG	Biotinylated secondary antibody	Sigma #B7264
Streptavidin-linked Cy5	Fluorescent tertiary antibody	Amersham #PA45001

dye DAPI (4′,6-Diamidino-2-phenylindole; 1 μg ml^{-1}; Sigma #D9542) for 10 min.

2.4. Microscopy and image processing

Labelled sections were mounted with Citifluor (Citifluor Ltd, UK), then coverslipped and sealed with nail varnish. The slides were initially viewed with a Leica DMRA microscope at 40 × magnification (Leica Microsystems GmbH, Germany), and digitally photographed with a Sensys KAF1401E digital camera system (Photometrics Ltd, USA) interfaced with a Compaq DeskPro personal computer (Compaq Computer Corp., USA) running V++ (Digital Optics Ltd, NZ).

Representative slides were then further imaged in three dimensions with either a Leica TCS 4d Confocal Microscope, or a Leica SP2 Confocal Microscope, using 40 × and 100 × objectives. The images were then transferred via an Ethernet network to a Macintosh G4 (Apple Computer Inc., USA) running Photoshop (Adobe Systems Ltd, USA).

The colour look-up tables for each of the images was altered according on the antibody and label used: keratocytes (CMFDA) were coloured green, nerves (Alexa-546) were coloured red, and other antibodies (Cy5) were labelled blue.

Specialised software developed in our laboratory ('microIMAGEBASE' (Brookes et al., 2001) was used to organise and interactively display the confocal data either as a maximum projection, a 90° rotation, or as a *z*-series.

3. Results

This study examined the corneas of 10 keratoconic individuals, and compared them with the corneas of three normal control individuals.

In the keratoconic tissue specimens, the degree of disease progression was determined by the proximity of the cone. The greatest destruction of normal corneal architecture was seen at the apex of the cone, and there was a gradient of diminishing damage toward the periphery. This study primarily focused on Bowman's layer, where nerves were seen to pass between epithelium and stroma.

All specimens were labelled first with the cell viability (esterase-activated) probe CMFDA, then with the antibody C3B9 that binds to acetylated α-tubulin. This antibody has proved to be an excellent nerve marker in this study, due to the high acetylated α-tubulin levels in the most stable microtubules present in the nerve axons. Although some sections were not labelled further, most sections were subsequently labelled with antibodies to integrin α3β1 (labels the nerves and basal epithelial cells) or Vimentin (a marker of cells of mesenchymal origin such as the keratocytes), or the intracellular proteolytic enzymes Cathepsin B and G. The cell nuclei in many sections were finally labelled with DAPI.

Despite the difficulty of simultaneously labelling a single tissue specimen with up to four probes, coupled with a range of ex vivo tissue states, all corneas examined showed a series of characteristic features.

3.1. Normal corneas

The architecture of the anterior cornea shows three well-defined tissue layers: Epithelium, Bowman's layer, and Stroma. Nerves passing between the anterior stroma and the epithelium, as seen in Fig. 1(A)–(C), were the only cellular structures found within the otherwise acellular Bowman's layer. The nerves often forked in a characteristic way before leaving the stroma, and were often in direct contact with the anterior keratocytes. Both the nerve and the basal epithelial cells labelled positively for the integrin α3β1, but not the stromal keratocytes (Fig. 1(D)–(F)), whereas antibodies to Vimentin labelled the nerves and the mesenchymally derived keratocytes, but not the epithelial cells.

The labelling patterns of both Cathepsin B and G seemed to be identical – the normal epithelium had a stronger labelling intensity for Cathepsin B and G than the keratocytes. The nerves also strongly labelled for Cathepsin B and G, in particular the nerve terminals. There was little or no positive keratocyte labelling for these Cathepsins (Fig. 1(J)–(L)).

3.2. Keratoconic corneas

The keratoconic corneas examined showed a gradient of disruption of the normal corneal architecture between the cone and the periphery of the excised button. Fig. 2(A)–(D) shows some of the earliest signs of keratoconic disruption, with the anterior keratocytes displaced slightly anteriorly into Bowman's layer at the point where the nerve passes through (this is particularly visible in the DAPI channel—Fig. 2(C)). The nuclei of several anterior keratocytes were also seen wrapping around the nerve, though close examination of the confocal *z*-series showed no direct connection between the nerve terminals and the basal epithelial cell nuclei, only the cell membranes and intercellular spaces.

Labelling the integrin α3β1 and Vimentin did not show any features that were markedly different to those seen in the normal cornea. The nerves and the basal epithelial cells labelled positively to the integrin α3β1, but not the stromal keratocytes (Fig. 2(E)–(H)). The nerves labelled more intensely than the basal epithelium. In contrast, antibodies to Vimentin principally labelled the nerves, but not the epithelial cells (Fig. 2(I)–(L)). However, the combination of integrin α3β1 and Vimentin was useful for determining the cell/layer fate when the normal architecture was disrupted in more advanced keratoconus.

More interesting results were obtained when labelling the intracellular Cathepsins. Fig. 2(M)–(P) shows an extensive nerve plexus ramifying as it passes through Bowman's

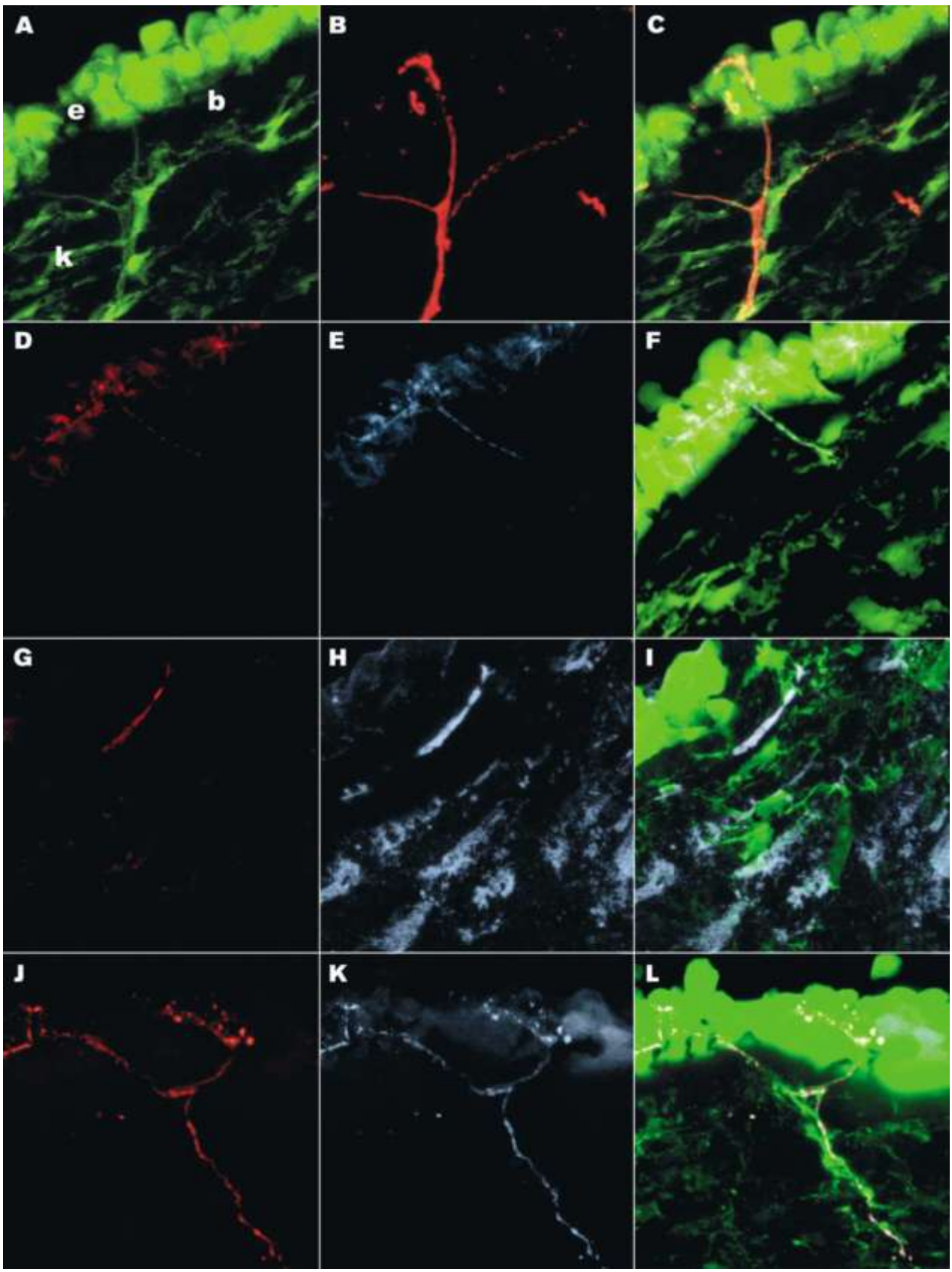
A
e
b
k
B
C
D
E
F
G
H
I
J
K
L

layer. The main nerve branch is seen travelling over 300 μm within the basal epithelium parallel to the anterior surface of Bowman's layer, which exhibits some spatial disruption. The DAPI channel in particular (Fig. 2(O)) shows anterior keratocyte cell nuclei displaced anteriorly, wrapped around the nerve plexus within it. Antibodies to Cathepsin B have strongly labelled the epithelium, when compared to the stroma, yet some (but not all) of the keratocytes, particularly those within Bowman's layer, are also expressing high levels. Furthermore, the squamous layer at the surface of the epithelium can be seen sloughing off, directly anterior to the Bowman's layer disruption.

At higher magnification, Fig. 3(A)–(D) shows a nerve branching as it passes through Bowman's layer, which has also been displaced anteriorly. As with Cathepsin B in Fig. 2(N), antibodies to Cathepsin G (Fig. 3(B)) have mostly labelled the epithelium, but also show strong labelling associated with the anterior keratocytes, particularly the cells associated with the nerve as it passes between the layers. Again, several keratocyte cell nuclei can be seen wrapping around the nerve as it passes through the stroma (Fig. 3(C)). Significantly, a small nerve thickening (~10 μm) is visible between the basal epithelial cells in the merged image (Fig. 3(D)), in close association with the neighbouring epithelial cell nuclei, which show intense Cathepsin G labelling. These nerve thickenings were seen to some degree in eight of the 10 keratoconic buttons examined in this study.

A more advanced destructive state of the epithelial–Bowman's layer–stromal complex can be seen in Fig. 3(E)–(H). Bowman's layer in the centre of the image is completely lost and is filled with keratocytes. Associated with this destruction is a large nerve thickening (~20 μm) within the basal epithelium that is very closely associated with the surrounding epithelial cell nuclei in the merged image (Fig. 3(H)). This thickening seems to be the termination of a long ramifying nerve that can be seen passing over 70 μm within the basal epithelial cells in this image.

Fig. 3(I)–(L) shows an example of a scarred keratoconic cornea exhibiting greater disease progression than in Fig. 3(E)–(H). Again, Bowman's layer is completely lost and filled with keratocytes, thereby directly connecting the keratocyte network to the epithelium. As in Fig. 3(F)/(H), a nerve can be seen winding through the basal epithelium (Fig. 3(J)), and appears to pass out of the epithelium and into the keratocyte network in the merged image (Fig. 3(L)). A nerve thickening (~10 μm) can be seen at the anterior margin of an intercellular space in the basal epithelial layer (Fig. 3(J)). Antibodies to Cathepsin G have labelled the nerve and also the keratocytes within the epithelial indentation (Fig. 3(K)).

4. Discussion

This study adds to our previous work (Sherwin et al., 2002), which examined the nature of keratoconus at a micro-anatomical level. In this earlier study, we showed discrete incursion of fine keratocyte processes into Bowman's layer, often in association with epithelial dimpling. We also found elevated levels of Cathepsin B and G expressed in keratocytes adjacent to these structural disruptions, and also in isolated cells or groups of cells deeper in the stroma. This current study builds on these observations, and explores the sequence of events occurring as the disease progresses, particularly in relation to the corneal nerves.

There are a number of caveats to bear in mind when examining this visual evidence. Firstly, all the tissue used in this study is of human origin. As there is no animal model of keratoconus, the only source of keratoconic tissue is corneal buttons removed at the time of penetrating keratoplasty. Patients only undergo this operation when they have advanced keratoconus and are suffering severe visual and/or structural problems. Hence, it is difficult to ascertain the exact sequence of steps involved in the progression of the disease, as every keratoconic button contains many stages of destruction and healing simultaneously. Secondly, normal control human tissue can only be obtained after death, so is often exhibiting confounding post-mortem

Fig. 1. Normal cornea. (A–C) Antero-posterior view of the anterior cornea, showing a typical nerve passing between the anterior stroma and the epithelium, through Bowman's layer (b). The keratocytes (k) and epithelium (e) are labelled with CMFDA (A). The nerve is labelled with the antibody C3B9 (B), and forks in a characteristic way before leaving the stroma, where it is lying in very close association with an anterior keratocyte (composite CMFDA/nerve image—C). A smaller nerve side branch passes directly through the keratocyte, before travelling within the anterior keratocyte network parallel with Bowman's membrane. $X/Y = 100$ μm; $Z = 28{\cdot}05$ μm (28 optical sections). (D–F) Antero-posterior view of the anterior stroma and epithelium showing the distribution of integrin α3β1. A nerve labelled with antibody C3B9 (D) penetrates a keratocyte before passing through Bowman's layer, and branches extensively within the basal epithelial cells). Both the nerve and the basal epithelial cells have labelled positively of the integrin α3β1 (E), but not the stromal keratocytes. CMFDA labelling (composite nerve/integrin α3β1 image—F) shows the keratocytes and epithelium. $X/Y = 100$ μm; $Z = 20{\cdot}93$ μm (21 optical sections).(G–I) Antero-posterior view of the anterior cornea showing the Vimentin labelling pattern. In this normal cornea, an antibody to Vimentin (H) labels the nerves (G) and the mesenchymally derived keratocytes, but not the epithelial cells. The relationship between the cells and the nerves can be seen in the composite nerve/Vimentin image (I). $X/Y = 100$ μm; $Z = 15{\cdot}98$ μm (16 optical sections). (J–L) Antero-posterior view of the anterior view Cathepsin G labelling in the normal cornea. A nerve labelled with C3B9 (J) passes through a large distance (~50 μm) of anterior keratocyte network, in very close association with the keratocytes (green in composite nerve/Cathepsin G image—L). Before passing through Bowman's membrane, the nerve branches and ramifies extensively within the epithelium, ending in a series of beaded terminals. Note that the normal epithelium has a stronger labelling intensity for Cathepsin G than the keratocytes (K). The nerve is also strongly labelled, particularly the nerve terminals. The labelling patterns of both Cathepsin B (not shown) and G are very similar. $X/Y = 100$ μm; $Z = 21{\cdot}6$ μm (22 optical sections).

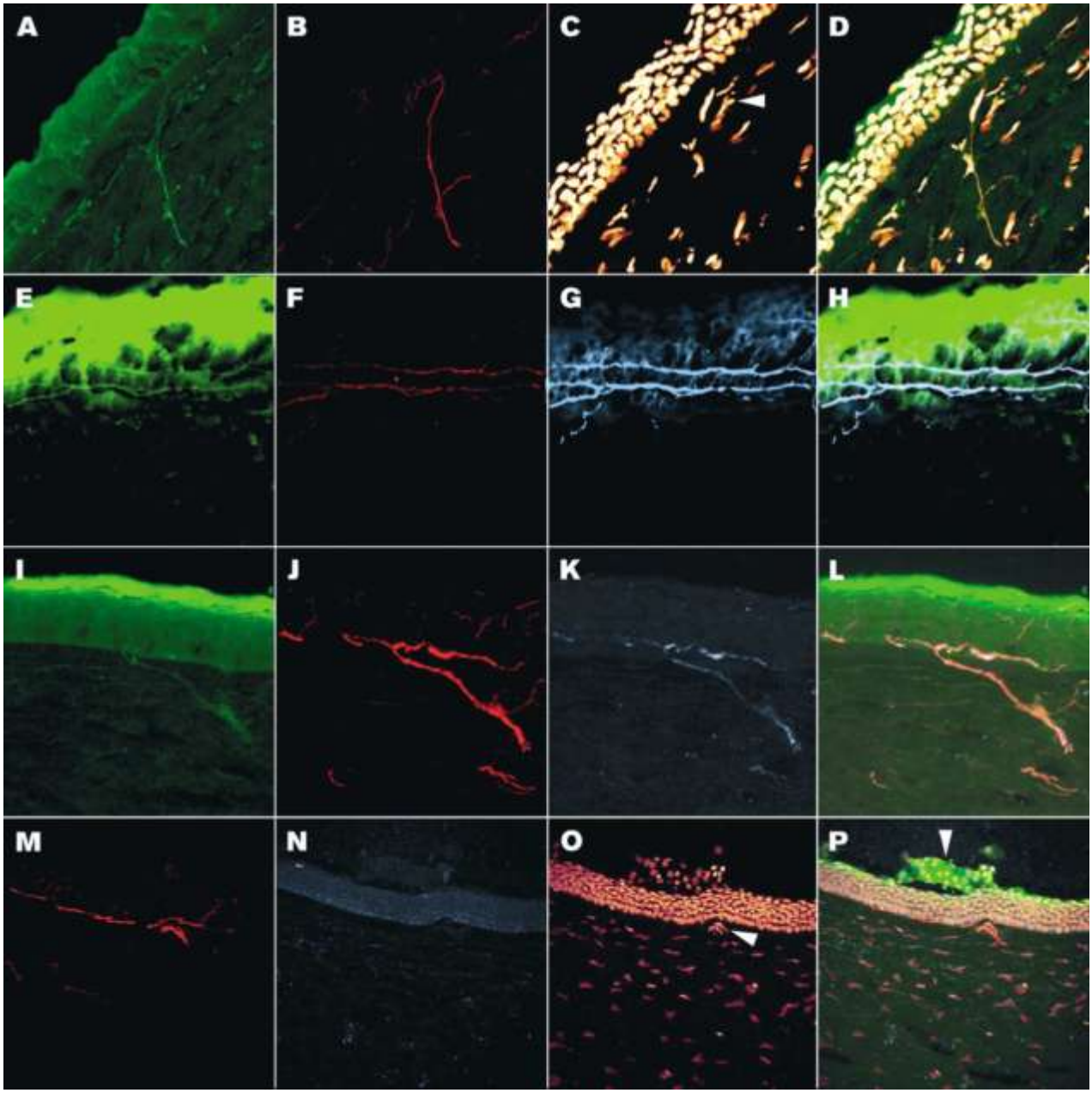

Fig. 2. Keratoconic cornea. (A–D) Antero-posterior view of the anterior keratoconic cornea. A nerve labelled with C3B9 (B) passes at least 100 μm between the stroma and the epithelium labelled with CMFDA (A—and composite CMFDA/nerve/DAPI image—D). Various smaller nerves can be seen branching off the main trunk as it passes through the stroma. The main nerve also branches as it passes through Bowman's membrane, and then ramifies extensively within the basal epithelial cells. There is some spatial disturbance of the anterior keratocyte layer at the point where the nerve passes through, as seen in the CMFDA channel (A—and composite CMFDA/nerve/DAPI image—D), but particularly in the DAPI channel (C), where the nuclei of several anterior keratocytes can be seen wrapping around the nerve (arrow). However, examination of the confocal *z*-series generating this image shows that there does not appear to be any direct connection between the nerve terminals and the basal epithelial cell nuclei (not shown). $X/Y = 187{\cdot}5$ μm; $Z = 39{\cdot}69$ μm (40 optical sections). (E–H) Lamellar view of the anterior keratoconic cornea (CMFDA—E), where a integrin α3β1 (G) have labelled both the nerve (F) and the basal epithelial cells (E). The nerve however, has labelled more intensely than the epithelium. Two long branching nerve trunks can be seen passing in parallel across the image (250 μm) at the level of the basal epithelial cells (composite CMFDA/nerve/integrin α3β1 image—H). $X/Y = 250$ μm >; $Z = 16{\cdot}25$ μm (16 optical sections). (I–L) Antero-posterior view of the anterior keratoconic cornea, showing antibody labelling to Vimentin (K), which labels the nerve in particular. The keratocytes in this image have poor esterase (CMFDA—E) and Vimentin (K) labelling. The nerve labelled with antibody C3B9 (J) passes through 120 μm of anterior stroma, branching along the way, before passing through what remains of Bowman's membrane, and then ramifying extensively within the basal epithelium. As in Fig. 2(E)–(H), the nerve travels within the basal epithelium for some distance (~200 μm) (composite CMFDA/nerve/Vimentin image—L). $X/Y = 200{\cdot}32$ μm; $Z = 29{\cdot}71$ μm (30 optical sections). (M–P) Antero-posterior view of the anterior keratoconic cornea, showing antibody labelling to Cathepsin B. An extensive nerve thickening labelled with antibody C3B9 ramifies as it passes through Bowman's membrane (M). The main nerve branch can then be seen travelling over 300 μm within the basal epithelium parallel to the anterior surface of Bowman's membrane. This layer itself is exhibiting some spatial disruption—the DAPI channel in particular shows anterior keratocyte cell nuclei displaced anteriorly,

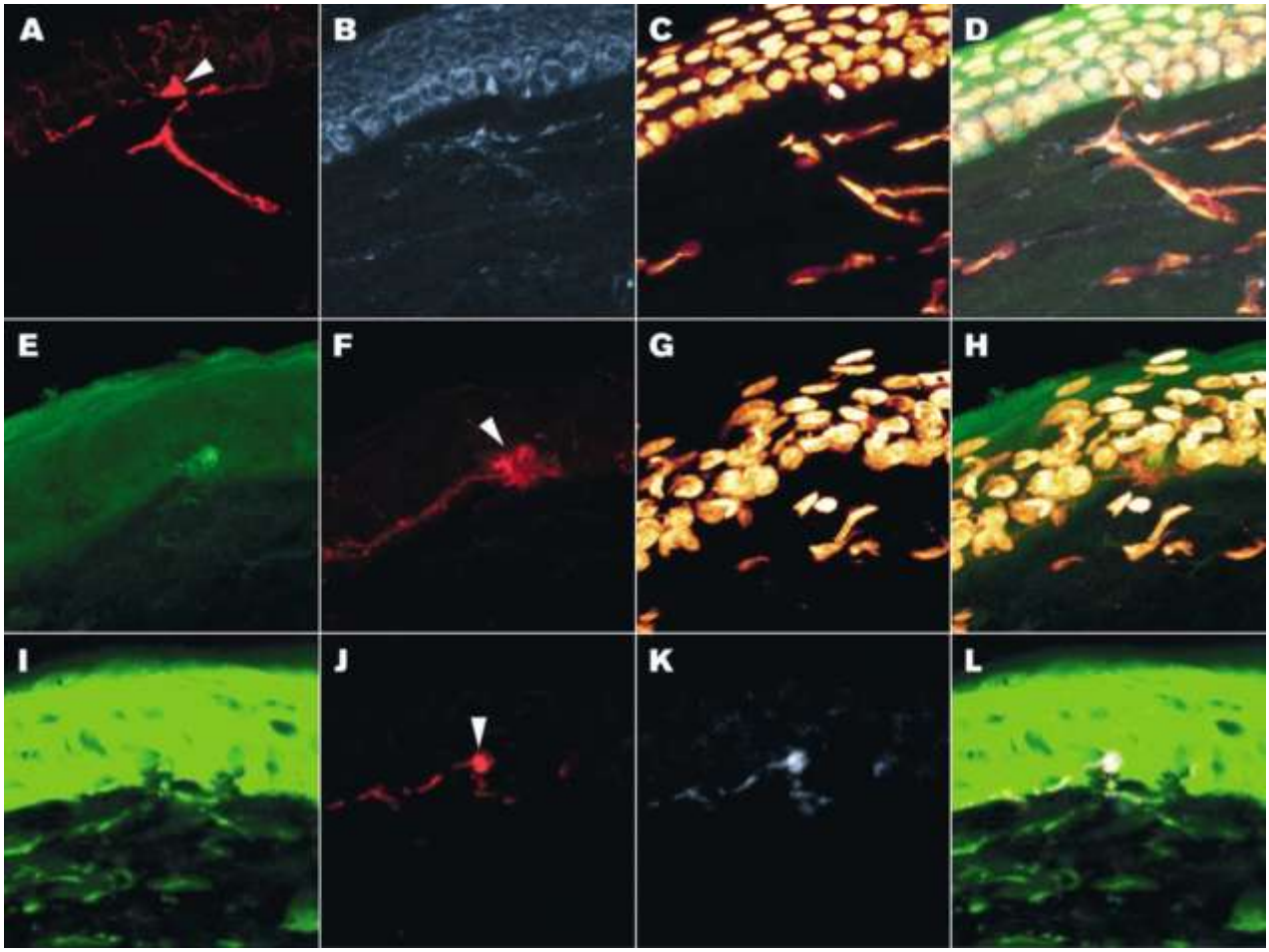

Fig. 3. Keratoconic epithelial nerve thickening. (A–D) Antero-posterior view of the anterior keratoconic cornea, showing similar features as Fig. 2(M)–(P) but at a higher magnification, particularly the development of a localised nerve thickening. A nerve labelled with antibody C3B9 (A) branches as it passes through Bowman's membrane, which has been displaced anteriorly. Antibodies to Cathepsin G (B) have mostly labelled the epithelium, but there is strong labelling associated with the anterior keratocytes, particularly the cells associated with the nerve as it passes between the layers. Several keratocyte cell nuclei labelled with DAPI (C) can also be seen wrapping around the nerve as it passes through the stroma. A small nerve thickening (~10 μm) is visible between the basal epithelial cells (arrow—A), in close association with the neighbouring epithelial cell nuclei, which is expressing Cathepsin G (composite nerve/Cathepsin G/DAPI image—D). $X/Y = 105$ μm; $Z = 38{\cdot}95$ μm (30 optical sections). (E–H) Antero-posterior view of the anterior keratoconic cornea, showing a more advanced destructive state of the epithelium–Bowman's layer–stroma complex. Bowman's membrane in the centre of the image is completely lost, and contains keratocytes (labelled with CMFDA—E or DAPI—G). Associated with this destruction is a large nerve thickening (~20 μm) labelled with antibody C3B9 (arrow—F) within the basal epithelium that is very closely associated with the surrounding epithelial cell nuclei (G and composite CMFDA/nerve/DAPI image—H). This thickening seems to be the termination of a long ramifying nerve that can be seen passing over 70 μm through the basal epithelial cells. $X/Y = 93{\cdot}75$ μm; $Z = 42{\cdot}54$ μm (20 optical sections). (I–L) Antero-posterior view of the anterior keratoconic cornea, showing even greater disease progression than in Fig. 3(E)–(H). CMFDA labelling (I) shows that Bowman's membrane is completely lost and filled with keratocytes, thereby connecting the keratocyte network to the epithelium. A nerve labelled with antibody C3B9 (J) can be seen winding through the basal epithelium, which then appears to pass out of the epithelium and into the keratocyte network. A nerve thickening (~10 μm) can be seen at the anterior margin of a hole in the basal epithelial layer (arrow). Antibodies to Cathepsin G (K) have labelled the nerve and the also the keratocytes within the epithelial indentation (composite CMFDA/nerve/Cathepsin G image—L). $X/Y = 105$ μm; $Z = 6{\cdot}64$ μm (six optical sections).

changes, particularly to the nerve architecture, which degrades quickly after death. However, fine detail of the nerves, such as the beading seen in Fig. 1(B), correlates well with similar structures seen in the human in vivo (Grupcheva et al., 2002). Thirdly, attempting to label tissue with up to four probes simultaneously can sometimes be problematic, and perfect labelling of a single tissue section with multiple probes is not always possible.

Keratoconus progresses as a combination of simultaneously destructive and healing processes (Rabinowitz,

wrapping around the nerve plexus within it (O—arrow). Antibodies to Cathepsin B (N) have strong labelling in the epithelium when compared to the stroma, yet some of the keratocytes are also expressing high levels, particularly those within Bowman's membrane. Note that not all of the keratocytes in this section are associated with Cathepsin B expression. The anterior layer of the squamous epithelium can be seen sloughing off, directly above the Bowman's membrane disruption (arrow in composite nerve/Cathepsin B/DAPI image—P). $X/Y = 375$ μm; $Z = 35{\cdot}17$ μm (20 optical sections).

1998). Central to this current study is the observation that disruptions of Bowman's layer often occur at the point where nerves pass between the stroma and the epithelium. Whilst no attempt was made to quantify the role the nerves play in the progression of keratoconus, they were seen to be involved in the disease process in some way in all 10 keratoconic corneas examined in this particular study. There is also compelling qualitative evidence shown here suggesting that this destructive process involves the nerves or their associated Schwann cells, which express the proteolytic enzymes Cathepsin B and G (and possibly others). The nerves in the normal cornea also express these enzymes, but not nearly as extensively as during active keratoconus. There is no literature examining cathepsin expression in corneal nerves so this may be a novel finding, but these enzymes are known to be active in other diseased neural tissues, particularly during brain tumour invasion (Levicar et al., 2002).

Early in the destructive process, the nerve becomes a locus for a thickening within the basal epithelium (Fig. 3(A)). It is associated with high levels of Cathepsin B and G along with the neighbouring epithelial cells, and appears to become larger and more destructive as the disease progresses (Fig. 3(B), (F) and (J)). Although some degree of epithelial nerve thickening was visible in eight of the 10 keratoconic buttons examined, they were not always easy to find and may well have been missed in previous studies. A more thorough quantitative survey of a series of keratoconic corneas is needed to answer this definitively.

In addition to their sensory functions, corneal nerves exert many important trophic effects on the cornea, including maintenance of epithelial integrity, modulation of cell proliferation and mitosis, stimulation of ion transport, and regulation of wound healing after corneal injuries (Belmonte et al., 1996). The actual mechanisms by which the nerves exert these effects is not fully understood, but several biological active neuropeptides such as Substance P, Calcitonin gene-related peptide, and Neurotensin have been implicated in this role (Bourcier et al., 2002).

As shown previously, the anterior keratocytes in both normal and keratoconic corneas lie in very close association to the nerves (Müller et al., 1996). At the confocal microscope level, their nuclei and cytoplasm appear to wrap around the nerve as it passes through the stroma (Figs. 2(D), (P) and 3(D) and (H)). In keratoconus, it is these keratocytes in particular that begin to express high levels of destructive enzymes, and it seems that eventually this entire epithelium–nerve–keratocyte complex may internally digest the surrounding extracellular matrix (Figs. 2(P) and 3(D)).

This process of extracellular matrix 'remodelling' is known from other connective tissues (Everts, 1995, 1996; Creemers et al., 1998; Kerkvliet et al., 1999), and it seems pertinent to introduce this literature into the keratoconus discussion, as the current understanding of this process fits the observations made here and elsewhere in the keratoconus literature well.

The process probably begins when the keratocyte cell processes attach to extracellular matrix ligands through their integrin receptors. The fenestrations seen in electron micrographs of the keratocyte cell membranes may be the actual attachment sites (Müller et al., 1995). This binding may initiate a cascade of events, including a rearrangement and reorganisation of elements of the cytoskeleton, in particular the microfilament system, as well as an increased expression and release of Gelatinase A/Stromelysin. Cell processes surround the fibril, and a microenvironment is created between the engulfing membrane and the enclosed fibril. Within this intimate milieu, membrane-bound enzymes (Gelatinase A (MMP-2)/Stromelysin) partially digest the collagen fibril and/or its associated components. The microfibrillar Collagen Type VI, for example, is predigested by serine proteinases (e.g. Cathepsin G). This action results in fragmentation of the fibril and its uptake into a phagosome, mediated by Interleukin-1α (there is known to be a large increase in the number of Interleukin-1α (Bureau et al., 1993), which inhibit the intracellular phagocytic pathway, whilst simultaneously promoting extracellular digestion by inducing the release of collagenolytic enzymes like collagenase) and TGF-β (which has the opposite effect). The lysosomes then fuse with the phagosomes, and further breakdown is accomplished within this acidified environment. First the proteinaceous core surrounding the fibril is digested, and then the resulting fibrillar structures are degraded under the influence of enzymes such as the cysteine proteinases (e.g. Cathepsin B), resulting in the production of the breakdown product hydroxyproline.

Additionally, epithelial cells are also known to participate in the remodelling process in other connective tissues (Birek et al., 1980; Salonen et al., 1991). In the cornea, it is interesting to note that from the first detailed study of keratoconus using electron microscopy (Teng, 1963), the earliest observable pathology was seen in the basal epithelial cells. It appeared then as though these cells released proteolytic enzymes, which attacked the adjacent stroma. In the basal epithelial cells Teng (1963) saw disorganisation of the organelles, in particular the endoplasmic reticulum and the Golgi system. Degeneration of Bowman's layer continued until the formation of a new epithelial basement membrane, presumably through up-regulating the production of basement membrane proteins (Collagen $\alpha_{1/2}$ IV chains/Laminin-1/Laminin-5) (Stepp et al., 1993; Tuori et al., 1997). However, the more epithelial cells that survive this process, the more stromal damage that is done. In our previous paper (Sherwin et al., 2002), we determined that the epithelial ingrowths were dimples, rather than ridges or fissures, further supporting the idea that these disruptions may occur around a single nerve fibre.

As the disease progresses and Bowman's layer is totally digested, the keratocytes are pushed progressively

anteriorly and eventually contact the epithelium, which grows down into the digested hole (Kanai, 1968) whilst continually trying to maintain a smooth and continuous exterior surface (Hanne et al., 1989). Digested and internalised extracellular matrix may pass eventually into the thickened epithelium, where it is shed with the squamous layer (Fig. 2P). In this way, deeper and deeper layers of the cornea are gradually destroyed. As this destructive 'remodelling' process is occurring, the cornea is simultaneously undergoing a wound healing response, but ultimately degradation overcomes restoration, and a scarred cone forms.

In summary, it seems that keratoconus may progress by groups of anterior stromal keratocytes successively disassociating themselves from the rest of the keratocyte network, and entering a destructive extracellular matrix-remodelling phase as part of a greater cycle of wound-healing. Corneal wound healing is known to be initiated by epithelial injury followed by keratocyte activation via cytokine diffusion (for a review see Wilson et al., 2001). In this study we show nerves crossing Bowman's layer and lying very closely to both keratocyte and epithelial cell nuclei. It is therefore possible that they form a second trans-Bowman's communication pathway, albeit cellular rather than extracellular. Furthermore, we observed both keratocytes expressing high levels of Cathepsin B and G, and varying degrees of corneal damage at these sites of nerve crossing. It is not clear from this study whether the nerves themselves (or their Schwann cells) are inherently destructive, yet they are associated with higher levels of Cathepsin B and G expression. It seems possible that the nerves may be mediating a feedback mechanism of epithelial initiation and keratocyte activation, trapping the cornea in a destructive cycle of matrix remodelling and wound healing.

Our previous study (Sherwin et al., 2002) identified an early event in the pathogenesis of keratoconus as the invasion of Bowman's layer by keratocytes and epithelial cells. This study shows that corneal nerve fibres crossing Bowman's layer are also implicated in this feature of keratoconic pathology, and indeed may be facilitating the direct keratocyte–epithelial interactions in this disease. Further studies are required to elucidate the molecular involvements between keratocytes, nerve fibres and epithelium, to determine the molecular basis of the pathogenesis of keratoconus.

Acknowledgements

The authors would like to acknowledge the help of the New Zealand National Eye Bank in supplying normal tissue and financially supporting N. B., and many of the Auckland-based ophthalmic surgeons for the supply of keratoconic buttons. We would also like to thank the Auckland Medical Research Foundation, the National Keratoconus Foundation (USA), the University of Auckland Research Committee, and the New Zealand Lottery Grants Board for their financial support of this project.

References

Armitage, W.J., Moss, S.J., 1990. Storage of corneas for transplantation. In: Easty, D.L., (Ed.), Current Ophthalmic Surgery, Baillère Tindal, London, pp. 193–199.

Belmonte, C., Gallar, J., 1996. Corneal nociceptors. In: Belmonte, C., Cervero, F. (Eds.), Neurobiology of Nociceptors, Oxford University, Oxford, UK, pp. 147–183.

Birek, P., Wang, H.M., Brunette, D.M., Melcher, A.H., 1980. Epithelial rests of Malassez in vitro. Phagocytosis of collagen and the possible role of lysosomal enzymes in collagen degradation. Lab. Invest. 43, 61–72.

Bourcier, T., Rondeau, N., Paquet, S., Forgez, P., Lombet, A., Pouzaud, F., Rostène, W., Borderie, V., Laroch, L., 2002. Expression of neurotensin receptors in human corneal keratocytes. Invest. Ophthalmol. Vis. Sci. 43, 1765–1771.

Brookes, N.H., Sherwin, T., Loh, I.-P., Poole, C.A., Clover, G.M., 2001. Interactive multimedia to study corneal keratocyte structure and function. Microsc. Anal. 23, 5–7.

Bureau, J., Fabre, E.J., Hecquet, C., Pouliquen, Y., Lorans, G., 1993. Modification of prostaglandin E2 and collagen synthesis in keratoconus fibroblasts, associated with an increase of interleukin 1 alpha receptor number. Sciences de la Vie Comptes Rendus de L'Academie des Sciences—Serie III 316, 425–430.

Clover, G.M., Brookes, N.H., Poole, C.A., 1996a. Confocal laser scanning microscopy of human corneal keratocytes with co-localised membrane gap junction proteins. Invest. Ophthalmol. Vis. Sci. 37, S1013.

Clover, G.M., Brookes, N.H., Poole, C.A., 1998. Simultaneous co-localisation of keratocytes and connexins 43 and 50. Invest. Ophthalmol. Vis. Sci. 39 (4), S453.

Clover, G.M., Poole, C.A., Brookes, N.H., 1996b. Confocal imaging of gap junction protein associated with the keratocytes of the human cornea. Aust. NZ. J. Ophthalmol. 24, 10–12.

Creemers, L.B., Jansen, I.D., Docherty, A.J., Reynolds, J.J., Beerstsen, W., Everts, V., 1998. Gelatinase A (MMP-2) and cysteine proteinases are essential for the degradation of collagen in soft connective tissue. Matrix Biol. 17, 35–46.

Everts, V., Korper, W., Niehof, A., Jansen, I., Beertsen, W., 1995. Type VI collagen is phagocytosed by fibroblasts and digested in the lysosomal apparatus: involvement of collagenase, serine proteinases and lysosomal enzymes. Matrix Biol. 14, 665–676.

Everts, V., van der Zee, E., Creemers, L., Beertsen, W., 1996. Phagocytosis and intracellular digestion of collagen, its role in turnover and remodelling. Histochem. J. 28, 229–245.

Grupcheva, C.N., Wong, T., Riley, A.F., McGhee, C.N.J., 2002. Lens and cornea assessing the sub-basal nerve plexus of the living healthy human cornea by in vivo confocal microscopy. Clin. Exp. Ophthalmol. 30, 187–190.

Hahnel, C., Somodi, S., Weiss, D.G., Guthoff, R.F., 2000. The keratocyte network of human cornea: a three-dimensional study using confocal laser scanning fluorescence microscopy. Cornea 19, 185–193.

Hanne, K.D., Pouliquen, Y., Waring, G.O., 1989. Corneal stromal wound healing in rabbits after 193 nm excimer laser surface ablation. Arch. Ophthalmol. 107, 895–901.

Jester, J.V., Barry, P.A., Lind, G.J., Petroll, W.M., Garana, R., Cavanagh, H.D., 1994. Corneal keratocytes: in situ and in vitro organisation of cytoskeletal contractile proteins. Invest. Ophthalmol. Vis. Sci. 35, 730–743.

Kanai, A., 1968. Electron microscopic studies of keratoconus. Nippon Ganka Gakkai Zasshi 72, 902–918.

Kerkvliet, E.H., Docherty, A.J., Beertsen, W., Everts, V., 1999. Collagen breakdown in soft connective tissue explants is associated with the level

of active gelatinase A (MMP-2) but not with collagenase. Matrix Biol. 18, 373–380.

Levicar, N., Strojnik, T., Kos, J., Dewey, R.A., Pilkington, G.J., Lah, T.T., 2002. Lysosomal enzymes, cathepsins in brain tumour invasion. J. Neuro-Oncol. 58, 21–32.

Marfurt, C.F., Ellis, L.C., 1993. Immunohistochemical localisation of tyrosine hydroxylase in corneal nerves. J. Comp. Neurol. 336, 517–531.

Müller, L.J., Pels, E., Vrensen, G.F.J.M., 1995. Novel aspects of the ultrastructural organisation of human corneal keratocytes. Invest. Ophthalmol. Vis. Sci. 36, 2557–2567.

Müller, L.J., Pels, E., Vrensen, G.F.J.M., 1996. Ultrastructural organisation of human corneal nerves. Invest. Ophthalmol. Vis. Sci. 37, 476–488.

Müller, L.J., Vrensen, G.F.J.M., Pels, E., Cardozo, B.N., Willekens, B., 1997. Architecture of human corneal nerves. Invest. Ophthalmol. Vis. Sci. 38 (5), 985–994.

Nishida, T., Yasumoto, K., Otori, T., Desaki, J., 1998. The network structure of corneal fibroblasts in the rat as revealed by scanning electron microscopy. Invest. Ophthalmol. Vis. Sci. 29, 1887–1887.

Ojeda, J.L., Ventosa, J.A., Piedra, S., 2001. The three-dimensional microanatomy of the rabbit and human cornea. A chemical and mechanical microdissection—SEM approach. J. Anat. 199, 567–576.

Petridou, S., Masur, S.K., 1996. Immunodetection of connexins and cadherins in corneal fibroblasts and myofibroblasts. Invest. Ophthalmol. Vis. Sci. 37, 1740–1748.

Poole, C.A., Brookes, N.H., Clover, G.M., 1993. Keratocyte networks visualised in the living cornea using vital dyes. J. Cell Sci. 106, 685–692.

Poole, C.A., Brookes, N.H., Clover, G.M., 1996. Confocal imaging of the keratocyte network in living porcine corneae using the fixable fluoroprobe 5-chloromethylfluorescein diacetate. Curr. Eye Res. 15, 165–174.

Poole, C.A., Brookes, N.H., Gilbert, R.T., Beaumont, B.W., Crowther, A., Scott, L., Merrilees, M.J., 1995. Detection of viable and non-viable cells in connective tissue explants using the fixable fluoroprobes 5-chloromethylfluorescein diacetate and ethidium homodimer-1. Connect. Tissue Res. 33, 233–241.

Rabinowitz, Y.S., 1998. Keratoconus. Surv. Ophthalmol. 42, 297–319.

Salonen, J., Uitto, V.J., Pan, Y.M., Oda, D., 1991. Proliferating oral epithelial cells in culture are capable of both extracellular and intracellular degradation of interstitial collagen. Matrix 11, 43–55.

Scharenberg, K., 1955. The cells and nerves of the human cornea. Am. J. Ophthalmol. 40, 368–379.

Sherwin, T., Brookes, N.H., Loh, I.-P., Poole, C.A., Clover, G.M., 2002. Cellular incursion into Bowman's membrane in the peripheral cone of the keratoconic cornea. Exp. Eye Res. 74, 472–483.

Snyder, M.C., Bergmanson, J.P.G., Doughty, M.J., 1998. Keratocytes: no more the quiet cells. J. Am. Optom. Assoc. 69, 180–187.

Spanakis, S.G., Petridou, S., Masur, S.K., 1998. Functional gap junctions in corneal fibroblasts and myofibroblasts. Invest. Ophthalmol. Vis. Sci. 39, 1320–1328.

Stepp, M.A., Spurr-Michaud, S., Gipson, I.K., 1993. Integrins in the wounded and unwounded stratified squamous epithelium of the cornea. Invest. Ophthalmol. Vis. Sci. 34, 1829–1844.

Teng, C.C., 1963. Electron microscopic study of the pathology of keratoconus. Am. J. Ophthalmol. 55, 18–47.

Tervo, T., 1977. Consecutive demonstration of nerves containing catecholamine and acetylcholinesterase in the rat cornea. Histochemistry 50, 291–299.

Tuori, A.J., Virtanen, I., Aine, E., Kalluri, R., Miner, J.H., Uusitalo, H.M., 1997. The immunohistochemical composition of corneal basement membrane in keratoconus. Curr. Eye Res. 16, 792–801.

Watsky, M.A., 1995. Keratocyte gap junctional communication in normal and wounded rabbit corneas and human corneas. Invest. Ophthalmol. Vis. Sci. 36, 2568–2576.

Wilson, S.E., Mohan, R.R., Mohan, R.R., Ambrósio, R. Jr., Hong, J., Lee, J., 2001. The corneal wound healing response: cytokine-mediated interaction of the epithelium, stroma, and inflammatory cells. Prog. Retin. Eye Res. 20, 625–637.